

# Desulfurization of the Ni(100) Surface Using Gas-Phase Hydrogen Radicals

Adam T. Capitano and John L. Gland\*

University of Michigan, Department of Chemistry, Ann Arbor, Michigan 48109-1055

Received: March 17, 1999; In Final Form: May 17, 1999

Gas-phase hydrogen radicals cause desulfurization of the sulfided Ni(100) surface even for temperatures as low as 120 K, resulting in H<sub>2</sub>S formation. In contrast, no thermal desulfurization is observed in the presence of coadsorbed hydrogen. During hydrogen radical exposure, sulfur is abstracted from the Ni(100) surface by a sequential Eley–Rideal mechanism. After hydrogen radical exposure, two additional H<sub>2</sub>S formation pathways involving coadsorbed hydrogen are observed during subsequent heating. In the first pathway, H<sub>2</sub>S formation is observed at 150 K, involving a partially hydrogenated intermediate formed during gas-phase atomic hydrogen exposure. The second pathway involves addition of desorbing subsurface hydrogen to adsorbed sulfur, leading to H<sub>2</sub>S formation at 190 K. Both the temperature and coverage dependence of the 150 K pathway support a sequential hydrogen addition mechanism with a sulfhydryl intermediate during temperature-programmed desorption (TPD) studies. Previous H<sub>2</sub>S decomposition studies on this surface show that the sulfhydryl intermediate is not stable above ~190 K because of thermal dehydrogenation. The temperature dependence of H<sub>2</sub>S formation and sulfur removal during exposure to the gas-phase hydrogen radical is also consistent with a sulfhydryl intermediate. Above 200 K, no desulfurization is observed during gas-phase hydrogen radical exposure. This thermal dehydrogenation of H<sub>2</sub>S also depends on the coverage of coadsorbed sulfur. Increasing sulfur coverages inhibits dehydrogenation of both H<sub>2</sub>S and SH. With higher sulfur coverages, H<sub>2</sub>S desorption is favored and substantial sulfur is removed during temperature-programmed reaction spectroscopy (TPRS) experiments after low-temperature hydrogen radical exposure. Taken together, the temperature- and coverage-dependent behavior indicates that sulfhydryl is an intermediate for sulfur abstraction. Through control of gas-phase hydrogen radical exposure, vacancies in sulfided nickel layers were generated. Hydrogen chemisorption studies were used to probe these sulfur vacancies. The new, low-temperature hydrogen desorption peak at 230 K corresponds to hydrogen modified by coadsorbed sulfur.

## Introduction

Poisoning of catalysts by sulfur is a serious problem to the chemical, petroleum, and automotive industries.<sup>1</sup> Regeneration of the catalyst is often possible through the removal of sulfur by hydrogen treatment at elevated temperatures and pressures.<sup>2</sup> However, these harsh conditions are both expensive and can induce sintering, which leads to reduced catalytic efficiency. Improved understanding of the fundamental mechanisms of hydrogen addition to adsorbed sulfur may lead to improved methods of catalyst desulfurization.

Previous mechanistic work has focused on understanding the chemistry of H<sub>2</sub>S adsorbed on metal surfaces.<sup>3</sup> For most of these surfaces, H<sub>2</sub>S exhibits the same general reactivity trends. At high coverages, physisorbed H<sub>2</sub>S desorbs below 150 K from metal surfaces. With heating, the remaining H<sub>2</sub>S dehydrogenates sequentially to form first a sulfhydryl (SH) and finally a sulfide layer. On several surfaces, SH intermediates have been characterized during H<sub>2</sub>S dehydrogenation.<sup>4,56</sup> If the resulting sulfide layer is heated in the presence of surface hydrogen, reaction to form H<sub>2</sub>S has not been observed below 10<sup>-4</sup> Torr.

Due to the large potential energy associated with the unpaired electron, gas-phase hydrogen radicals react with adsorbates that do not react with adsorbed hydrogen.<sup>7</sup> Hydrogen radicals have been used in a wide range of reactions including carbon–carbon bond activation in adsorbed cyclopropane,<sup>8</sup> hydrogenation of C=C bonds in adsorbed cyclohexene and ethylene,<sup>9</sup> reduction of adsorbed nitrogen to form ammonia,<sup>10</sup> and abstraction of

surface carbon through methanation.<sup>11</sup> In addition, gas-phase hydrogen radicals have been shown to populate subsurface hydrogen states in nickel surfaces.<sup>12</sup> With heating, this desorbing subsurface hydrogen has also been shown to be effective in inducing reactions near 200 K, even for adsorbates that are not susceptible to attack by surface hydrogen.

Because coadsorbed hydrogen does not induce H<sub>2</sub>S formation under ultrahigh vacuum (UHV) conditions, gas-phase hydrogen radicals provide an excellent means to probe sulfur hydrogenation. In this paper we show that gas-phase hydrogen radicals can form H<sub>2</sub>S by three mechanisms, including direct abstraction during exposure, formation of a SH intermediate, and by addition of subsurface hydrogen.

## Experimental Section

All experiments were performed in a UHV chamber equipped with turbo, ion, and TSP pumps that combined to give a base pressure of 5 × 10<sup>-10</sup> Torr. The system was equipped with a quadrupole mass spectrometer (QMS) for temperature-programmed reaction spectroscopy (TPRS), auger electron spectroscopy (AES) to verify surface cleanliness, and an atomic hydrogen source for the production of gas-phase atomic hydrogen.

A Ni(100) single metal crystal oriented within 0.5 degree of the low index plane was mounted on a ceramic support with two 0.5 mm tantalum wires that allowed heating to 1050 K and liquid nitrogen cooling to 110 K. The sample was attached to

an L-shaped manipulator that allows 3-coordinate displacements and 360° rotation. This setup allowed exact positioning in front of all instruments and gas dosers. Temperature was measured with a 0.01-mm chromel–alumel (type K) thermocouple spot welded to the back of the crystal. The crystal was cleaned by Ar<sup>+</sup> ion sputtering followed by annealing to 1000 K. AES was used to verify sample cleanliness.

All reactive gases were inlet through a directional dosing system controlled by a leak valve. Hydrogen (Matheson 99.9999%) and hydrogen sulfide (Matheson 99.5%) were used without further purification. All exposures are expressed in terms of Langmuirs (1 L =  $1 \times 10^{-6}$  Torr s) based on ionization gauge pressure readings and have not been corrected for large directional dosing fluxes and ion gauge sensitivity factors.

Gas-phase atomic hydrogen was generated by passing molecular hydrogen through a 2000 K tungsten tube that was heated by electron bombardment. The electrons for this process were created through thermionic emission from a tungsten filament. Both the filament and tube were housed in a stainless steel shroud that was water cooled to minimize the thermal load to the sample. During source operation, these precautions allowed a constant sample temperature of 120 K to be maintained. In each experiment, the hydrogen radical source was positioned 10 cm from the sample. Under these conditions, this source design was shown to have >90% efficiency for dissociation.<sup>13</sup> For the purposes of simplicity, we refer to the mixture of hydrogen atoms and molecules as gas-phase hydrogen radicals.

At the beginning of each experiment, a new sulfur-saturated Ni(100) surface was prepared. This sulfur-saturated surface with a known coverage of 0.5 ML was achieved through the thermal decomposition of H<sub>2</sub>S as described in detail by Anton.<sup>14</sup> Briefly, a clean Ni(100) surface is exposed to 2 L of H<sub>2</sub>S and then heated to 450 K to decompose the H<sub>2</sub>S and desorb all the hydrogen that forms. This procedure is repeated until no additional increase in the ratio of the S(152) to Ni(848) signal is detected by AES. Typically, three cycles were sufficient to achieve saturation.

The TPRS spectra were taken with a QMS adjusted to a low ionization energy of 30 eV to decrease the yield of hydrogen relative to organics. A Hunt Scientific control system allowed the simultaneous detection of up to eight masses with independent control of mass spectrum electron multiplier sensitivities. Desorption products were identified by prominent features in their mass spectrum fragmentation patterns.<sup>15</sup> For all experiments, a linear heating rate of 5 K/s was used.

Several sets of experiments were focused on sulfur removal during gas-phase hydrogen radical exposure by monitoring H<sub>2</sub>S formation. Because of experimental geometric constraints, the reacting surface and the mass spectrometer were not in a direct line of sight during the sulfur removal experiment. Reactivity measurements are based on the observed pressure of product H<sub>2</sub>S in the background. During these reactivity experiments, some drift associated with changes in the H<sub>2</sub>S pumping speed were observed as expected for a metal vacuum system. These pumping speed changes result in drift in measured background pressures for a fixed H<sub>2</sub>S flux (reactivity). Because of the uncertainty in H<sub>2</sub>S pumping speed, absolute reaction probabilities cannot be reliably calibrated over extended periods required for series of experiments. However, repeated experiments clearly demonstrate that accuracy was sufficient to determine relative trends in H<sub>2</sub>S background pressures measured

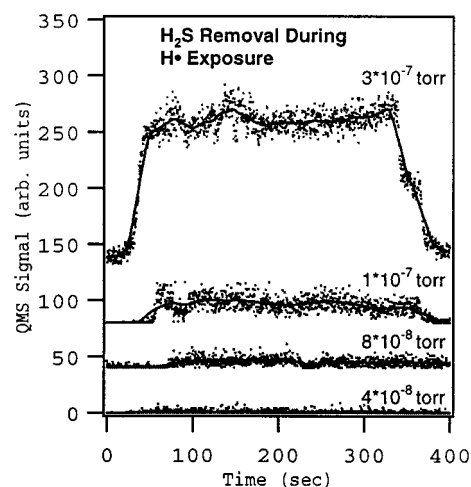


**Figure 1.** During exposure, gas-phase hydrogen radicals induce desulfurization of a Ni(100) surface by H<sub>2</sub>S formation. Increasing hydrogen radical pressure leads to more H<sub>2</sub>S formation.

reliably. In control experiments in which dihydrogen was exposed to a sulfur-saturated surface, hydrogen sulfide was not detected.

## Results

**Gas-Phase Hydrogen Radicals Abstract Sulfur from the Ni(100) Surface at 120 K.** Hydrogen sulfide background pressure intensity was monitored during gas-phase hydrogen radical exposure to a sulfur-saturated Ni(100) surface. As discussed in the *Experimental Section*, because of geometric constraints, no direct line of sight was available between the sample and mass spectrometer so H<sub>2</sub>S background pressure increases were used to characterize reactivity. The increase in H<sub>2</sub>S signal ( $m/e = 34$ ) as a function of gas-phase hydrogen radical pressure is shown in Figure 1. For even small gas-phase hydrogen radical pressures, sulfur is abstracted from the Ni(100) surface at 120 K. Increasing gas-phase hydrogen radical pressure results in increasing H<sub>2</sub>S background pressure, which indicates an increased rate of sulfur abstraction. The increased reaction rate scales approximately with hydrogen pressure, and the trends are very clear despite slow changes in pumping speed during experimental series. In contrast, control experiments in which dihydrogen is exposed to a sulfur-saturated Ni surface leads to no detectable H<sub>2</sub>S signal. This result is consistent with previous work that shows dihydrogen does not abstract sulfur from Ni at low pressures.<sup>16</sup>

Auger electron spectroscopy provides further support that gas-phase hydrogen radicals abstract sulfur from the Ni(100) surface. After dosing hydrogen radicals, the concentration of surface sulfur was measured by taking the ratio of the S(152) to the Ni(848) AES peaks. Sulfur coverage was determined by calibrating this ratio to the S/Ni ratio obtained from a saturated sulfur surface that is known to have a coverage of 0.5 ML.<sup>14</sup> From these ratios, the amount of sulfur remaining after gas-phase hydrogen radical exposures ranging from 0 to 168 L is shown in Figure 2. The reaction order is analyzed in Figure 9 in the *Discussion section*. For the largest gas-phase hydrogen radical dose we performed (168 L), ~90% of the surface sulfur was removed.

Additional desulfurization occurs when the surface is heated after gas-phase hydrogen radical exposure. Figure 3 shows the TPRS resulting from a sulfur-saturated Ni(100) that was exposed to 30 L of gas-phase hydrogen radicals. For the H<sub>2</sub>S TPRS trace ( $m/e = 34$ ), two peaks are observed at 150 and 190 K. In control

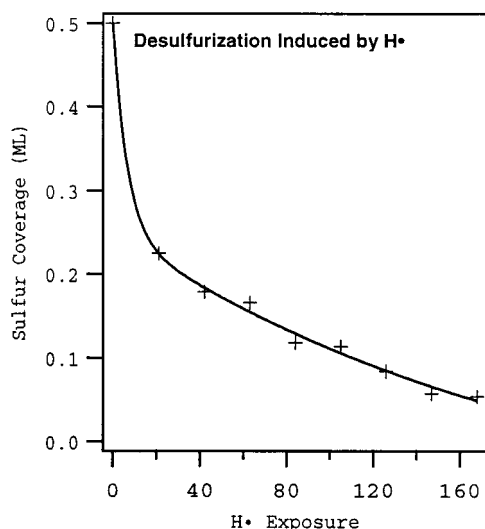


**Figure 2.** AES shows that increasing gas-phase hydrogen radical exposure to a saturated sulfur-covered Ni(100) surface leads to desulfurization. A 150 L exposure was sufficient to remove >90% of the surface sulfur.

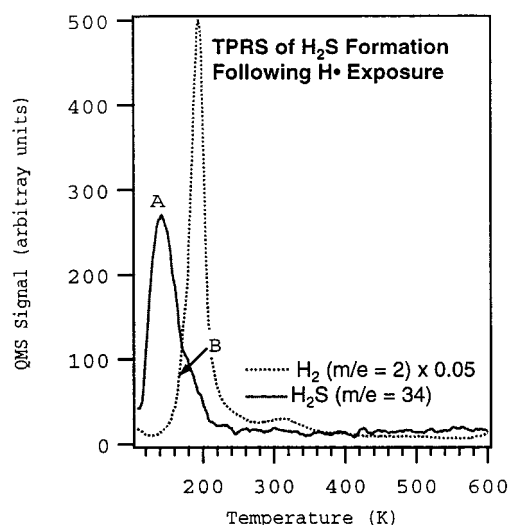


**Figure 3.** Heating the sulfided Ni(100) surface after hydrogen radical exposure leads to two H<sub>2</sub>S desorption peaks at 150 and 190 K in TPRS. The 150 K peak results from the hydrogenation of an SH intermediate formed during gas-phase hydrogen radical exposure. The 190 K peak is correlated with hydrogenation and desorption of subsurface hydrogen.

experiments with sulfur coadsorbed with *surface* hydrogen, neither feature is observed; therefore, these reactions must involve intermediates generated by the reaction of gas-phase hydrogen radicals with adsorbed sulfur. The hydrogen ( $m/e = 2$ ) TPRS spectra has two features at 190 and 310 K. The first peak results from desorbing subsurface hydrogen.<sup>17</sup> The second TPRS peak is from the recombination and desorption of surface hydrogen.<sup>18</sup>

Increasing exposure to gas-phase atomic hydrogen results in a *decrease* of H<sub>2</sub>S formation during subsequent TPRS. In Figure 4, H<sub>2</sub>S ( $m/e = 34$ ) TPRS following exposure of a sulfur-saturated surface to gas-phase hydrogen radicals in 20 L increments is shown. In each case, the two H<sub>2</sub>S desorption states at 150 and 190 K described in Figure 3 are observed. The most intense TPRS features are observed for the lowest (20 L) exposure. As gas-phase hydrogen radical dosage increases, the intensity of the TPRS peaks steadily decreases. Following a 160 L exposure, the amount of H<sub>2</sub>S desorbing decreases to 5% relative to the amount observed following a 20 L exposure.

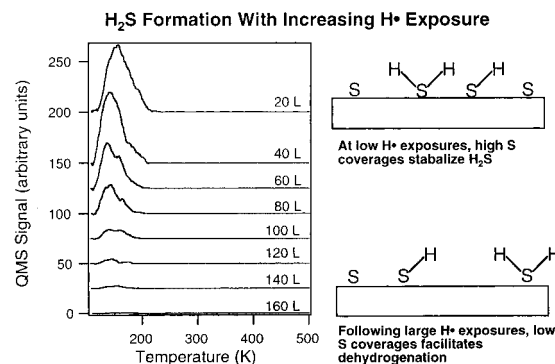


**Figure 4.** With increasing gas-phase hydrogen radical exposure, *less* H<sub>2</sub>S desorbs in subsequent TPRS experiments. Coadsorbed sulfur stabilizes H<sub>2</sub>S by site-blocking potential dehydrogenation reactions. Abstraction of sulfur (S) during hydrogen radical (H<sup>•</sup>) exposure makes surface conditions increasingly favorable for dehydrogenation.

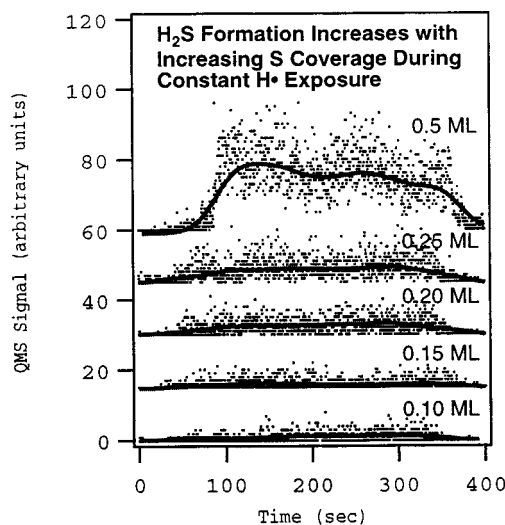


**Figure 5.** For a constant gas-phase hydrogen radical pressure of  $7 \times 10^{-8}$  Torr, increasing initial sulfur surface coverage leads to increasing H<sub>2</sub>S formation during hydrogen radical (H<sup>•</sup>) exposure. This sulfur (S) coverage dependence is consistent with the expected behavior of an SH intermediate.

With decreasing initial sulfur coverages on the Ni(100) surface, decreasing amounts of H<sub>2</sub>S are formed with constant gas-phase hydrogen radical pressure. In Figure 5, H<sub>2</sub>S formation for initial sulfur coverages ranging from 0.05 to 0.5 mL at a gas-phase hydrogen radical pressure of  $7 \times 10^{-8}$  Torr are shown. As the coverage of sulfur decreases, less H<sub>2</sub>S is detected in the mass spectrometer during hydrogen radical exposure. After each experiment, AES was used to determine the amount of sulfur remaining on the surface. When a saturated sulfur layer is exposed to a 20 L dose of gas-phase hydrogen radicals, >55% of the initial sulfur is removed. In contrast, when then initial coverage is 0.05 mL, only 8% of the sulfur is removed.

Figure 6 shows TPR spectra following a 30 L exposure of gas-phase hydrogen radicals to a saturated sulfide surface for temperatures ranging from 120 to 250 K. When the sample temperature is <150 K, the surface chemistry is similar to that described previously (Figure 3). For hydrogen radical exposures at higher surface temperatures, two differences are observed in subsequent H<sub>2</sub>S TPRS. With increasing sample temperature >150 K, the 190 K becomes increasingly dominant. With further increases in temperature, the 190 K peaks decrease in intensity until no H<sub>2</sub>S desorption is observed following exposure at 250 K. To measure the total amount of sulfur removed during the exposure and subsequent TPRS experiment, AES was used. For

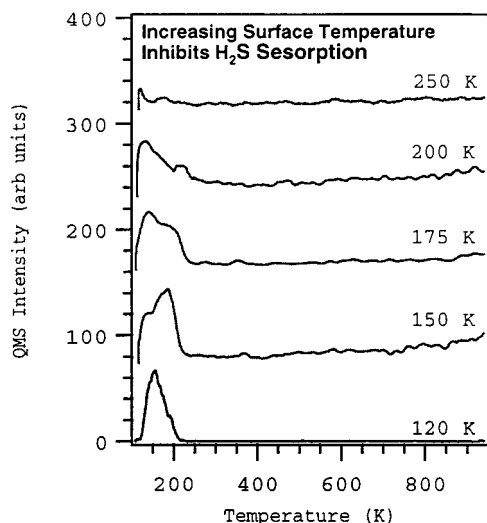


**Figure 6.** By increasing the surface temperature during gas-phase hydrogen radical exposure, less  $\text{H}_2\text{S}$  formation is observed in subsequent TPRS experiments. This thermal dependence of this process suggests an SH intermediate.

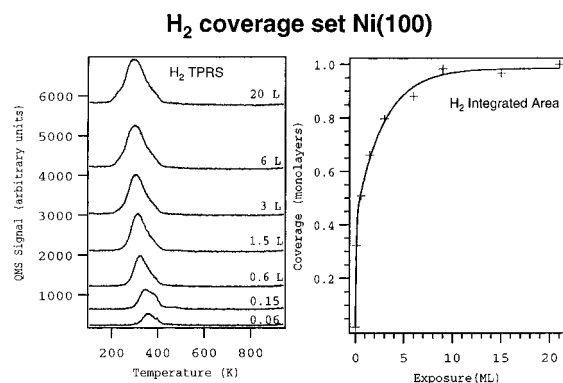


**Figure 7.** Coverage calibration of hydrogen desorption with TPRS. A 20 L exposure of dihydrogen was shown to be sufficient to saturate the Ni(100) surface giving a coverage of 1 mL.

sample temperatures  $> 250$  K, AES shows no decrease in surface sulfur coverage from hydrogen radical exposure (data not shown).

Adsorbed surface hydrogen has been used to characterize vacancies in the sulfur overlayer created with gas-phase hydrogen radicals. Hydrogen desorption from a clean Ni(100) surface was first characterized to establish hydrogen desorption temperatures and coverages. Hydrogen desorption from the clean Ni(100) surface for exposures ranging from 0.06 to 20 L of dihydrogen is shown in Figure 7a. Two desorption peaks centered near 270 and 300 K are the well-known  $\text{H}_2$   $\beta_1$  and  $\beta_2$  hydrogen desorption states.<sup>18</sup> With increasing exposure, the peak temperatures decrease as expected for second-order surface hydrogen recombination and desorption kinetics. An exposure of 20 L was sufficient to saturate the Ni(100) surface with hydrogen. The known 1 ML hydrogen saturation coverage<sup>19</sup> was used to establish the coverage scale for the exposure plot shown in Figure 7b.

A new, low-temperature hydrogen desorption peak results when hydrogen is exposed to a sulfur-covered surface with vacancies generated by gas-phase hydrogen radicals. In these experiments, a saturated sulfided Ni(100) surface was first exposed to gas-phase hydrogen radicals to create sulfur vacancies. This surface was annealed to 400 K to remove both subsurface and surface hydrogen. After annealing, the sample was cooled to 120 K and exposed to 20 L of dihydrogen and a

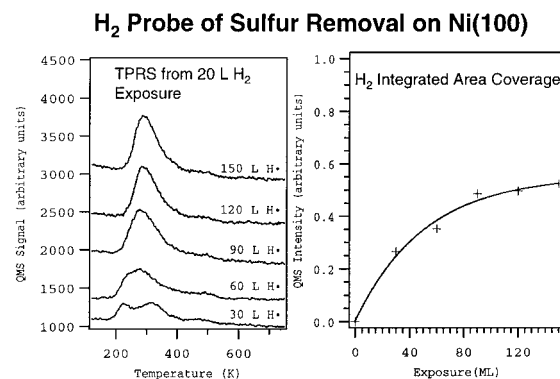


**Figure 8.** Vacancies in the sulfur overlayer created by gas-phase hydrogen radicals were characterized by hydrogen adsorption. Consistent with site blocking by coadsorbed sulfur, only partial monolayers of hydrogen desorb even though the surface was exposed to a 30 L dose of dihydrogen. For low vacancy concentration, a new hydrogen desorption state at 230 K is observed in the TPRS.

TPRS experiment was conducted. Figure 8a shows the results of the TPRS analysis conducted on surfaces for a range of gas-phase hydrogen radical exposures up to 150 L. For sulfur coverages of 0.15 ML (0.35 mL vacancies), a new  $\text{H}_2$  desorption feature is observed at 230 K in addition to the expected desorption near 300 K. As sulfur coverage decreases to 0.09 mL, this new feature decreases until it is no longer observed.

Despite the large exposure of dihydrogen, only partial monolayer coverages of hydrogen adsorb in the vacancies induced in the sulfided surface. By using the hydrogen calibration described in Figure 7b, concentrations of desorbing hydrogen could be obtained from the integrated areas of the hydrogen TPRS (Figure 8b). For the sulfided surface exposed to the 150 L of gas-phase hydrogen radicals, 0.58 ML of hydrogen adsorbed following a 30 L exposure of molecular hydrogen, indicating that adsorbed sulfur site blocks hydrogen adsorption.

## Discussion

Gas-phase hydrogen radicals effectively remove sulfur from the Ni(100) surface at temperatures as low as 120 K. As seen in Figure 2, even exposures as low as 20 L abstract  $> 40\%$  of the initial sulfur-saturated monolayer. As seen in Figures 1 and 5, adsorbed sulfur is removed as  $\text{H}_2\text{S}$  during hydrogen radical exposure. Because neither the adsorbed surface hydrogen nor gas-phase *dihydrogen* hydrogenate sulfur under these conditions, the 52 kcal/mol of potential energy supplied by the dissociation must provide the energy for reaction.<sup>16</sup> The BOC-MP calculations by Huntley have demonstrated that the reaction of surface hydrogen is thermodynamically unfavorable by 18 kcal/mol on nickel surfaces.<sup>20</sup> Gas-phase hydrogen radicals have a potential energy for reaction that is approximately an order of magnitude greater than surface hydrogen.<sup>21</sup> This large energy differential allows the thermodynamic barrier for  $\text{H}_2\text{S}$  formation to be overcome by gas-phase hydrogen radicals.

Sulfur abstraction from the surface is first order in sulfur surface coverage during gas-phase hydrogen radical exposure. In Figure 9, the natural log of surface sulfur concentration versus hydrogen radical exposure is plotted. The exponential decrease of the sulfur coverage indicates that the rate-determining step for the reaction of surface sulfur with hydrogen radicals follows first-order reaction kinetics. This result is consistent with several previous studies exploring the reaction kinetics of the reaction of gas-phase hydrogen radicals with adsorbates where first-order Eley–Rideal reaction kinetics are observed.<sup>22</sup> The rate constant



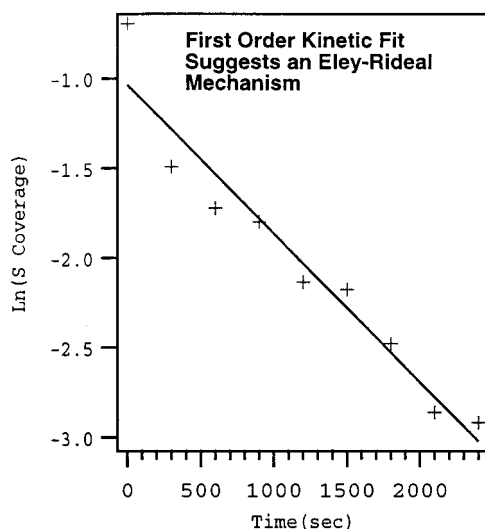


**Figure 9.** Desulfurization of the Ni(100) surface follows first-order reaction kinetics.

for the reaction was determined by a linear least-squares fit of the data to be 0.00036 mL/s for an atomic hydrogen flow, giving a background pressure of  $2 \times 10^{-7}$  Torr.

In addition to abstraction by direct reaction with hydrogen radicals by an Eley–Rideal mechanism, additional sulfur can be removed during subsequent heating by two additional mechanisms. When the surface is heated after gas-phase hydrogen radical exposure, two peaks at 150 and 190 K are seen in the  $\text{H}_2\text{S}$  ( $m/e = 34$ ) TPRS spectra (Figure 3). Comparison of the  $\text{H}_2\text{S}$  with the hydrogen TPRS trace shows that the large subsurface hydrogen desorption peak at 190 K corresponds with the  $\text{H}_2\text{S}$  190 K peak. It is well-known that desorbing subsurface hydrogen can hydrogenate adsorbates through a two-step process.<sup>23</sup> Subsurface hydrogen has an energy for reaction that is 15 kcal/mol higher relative to adsorbed surface hydrogen.<sup>24</sup> As subsurface hydrogen desorbs from the surface, substantial kinetic energy is focused in the  $z$ -direction<sup>25</sup> making it more reactive than surface hydrogen. Typically, desorbing subsurface hydrogen reacts with an adsorbate to form a partially hydrogenated intermediate in the first step. Then, surface hydrogen quickly adds to the intermediate leading to desorption. By analogy, we propose a similar mechanism for the reaction of desorbing subsurface hydrogen with sulfur adsorbed on the Ni(100) surface. In the initial reaction step, desorbing subsurface hydrogen attacks adsorbed sulfur to form SH. This SH is hydrogenated by surface hydrogen to form  $\text{H}_2\text{S}$ , which then desorbs.

The mechanism for  $\text{H}_2\text{S}$  formation and desorption at 150 K has been characterized by examining changes in the TPRS peak intensity as a function of gas-phase hydrogen radical exposure. As demonstrated in Figure 4, increasing gas-phase hydrogen radical exposure leads to decreasing  $\text{H}_2\text{S}$  desorption in both the 150 and 190 K desorption peaks. Studies of  $\text{H}_2\text{S}$  adsorption on the Ni(100) surface indicate that extensive dehydrogenation at low coverages of  $\text{H}_2\text{S}$  result in formation of surface sulfur.<sup>16</sup> With increasing coverage, neighboring sulfur and other sulfur-containing species inhibit dehydrogenation. As shown in Figure 2, gas-phase hydrogen radicals remove adsorbed sulfur during exposure. As hydrogen radical exposure increases, the average density of sulfur-containing species decreases. In the absence of adjacent site-blocking groups,  $\text{H}_2\text{S}$  or SH formed by reaction with gas-phase hydrogen radicals would be expected to dehydrogenate during subsequent heating, as observed for adsorbed  $\text{H}_2\text{S}$ .

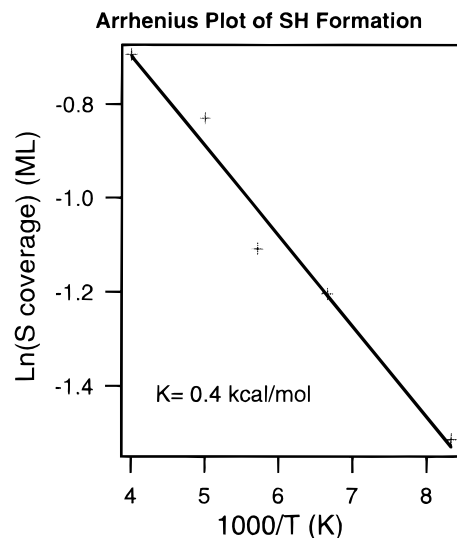


**Figure 10.** The activation energy for dehydrogenation of the SH intermediate was determined to be 0.4 kcal/mol using an Arrhenius plot. This low-energy barrier is consistent with the spontaneous dehydrogenation of SH observed on most metal surfaces.

The thermal stability for the process leading to the 150 K  $\text{H}_2\text{S}$  desorption peak is consistent with an adsorbed SH intermediate. By altering the temperature of the surface during gas-phase hydrogen radical exposure, the identity of the intermediate leading to the 150 K TPRS peak was probed. For surface temperatures up to 150 K, the amount of  $\text{H}_2\text{S}$  desorption observed in the following TPRS does not change significantly. Above this surface temperature, the amount of desorbing 150 K  $\text{H}_2\text{S}$  decreases rapidly whereas the amount of 190 K  $\text{H}_2\text{S}$  does not change significantly. This rapid decrease in the 150 K peak correlates with the known stability of SH intermediates. Previous work regarding  $\text{H}_2\text{S}$  adsorption and dehydrogenation on the Ni(100) surface suggested that an SH intermediate formed using electron energy loss spectroscopy (EELS).<sup>26</sup> The stability and reactivity of SH has been well characterized on the Pt-(111) surface.<sup>4</sup> Sulfhydryl was shown to react with surface hydrogen and form  $\text{H}_2\text{S}$  at temperatures as low as 170 K. This thermal data taken together with the coverage-dependent stability of the intermediate suggests that SH is the intermediate leading to  $\text{H}_2\text{S}$  formation and desorption at 150 K. An SH intermediate was also proposed recently by Rodriguez et al. who showed that gas-phase hydrogen radicals form  $\text{H}_2\text{S}$  on Ru(100) through an SH intermediate.<sup>27</sup>

The activation energy of SH dehydrogenation can be estimated using the temperature dependence of desulfurization during gas-phase hydrogen radical exposure. The hydrogenation of SH is rate limiting for the 150 K  $\text{H}_2\text{S}$  peak. In this temperature range, no significant  $\text{H}_2$  desorption occurs. Therefore, the decrease in amount of  $\text{H}_2\text{S}$  formed is directly related to the surface concentration of SH on the surface. An Arrhenius plot of the amount of  $\text{H}_2\text{S}$  formed is shown in Figure 10. From these data, an activation energy of 0.4 kcal/mol for SH decomposition is estimated. This low barrier is reflective of the spontaneous dehydrogenation of SH observed on most surfaces.<sup>3</sup>

Gas-phase hydrogen radicals remove surface sulfur to create vacancy sites in the sulfided overlayer in a controlled manner. The calibration curve shown in Figure 7b demonstrates that partial sulfur monolayers can be readily produced. Because defect sites in the basal plane of the sulfur overlayer in Ni/MoS<sub>2</sub> catalysts are thought to be the active site in HDS catalysts, methods for the creation of model systems is important.<sup>28</sup> Gas-phase hydrogen radicals do not modify the underlying surface

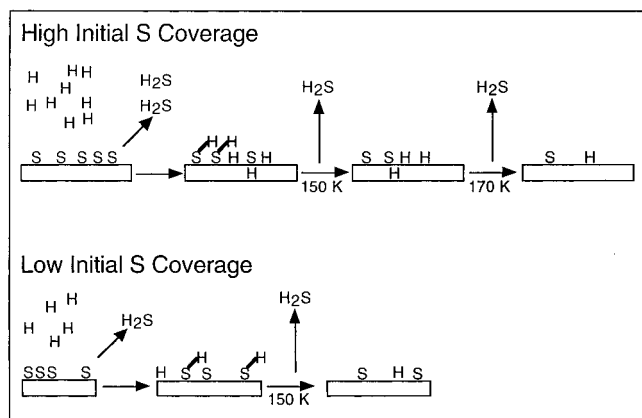


**Figure 11.** The proposed mechanism for desulfurization of the Ni(100) surface by gas-phase hydrogen radicals. During hydrogen radical ( $\text{H}^\bullet$ ) exposure, adsorbed sulfur is abstracted by  $\text{H}_2\text{S}$  formation that follows first-order reaction kinetics. When the surface is heated after exposure,  $\text{H}_2\text{S}$  desorbs from the surface at 150 and 190 K. The 150 K desorption state results from the hydrogenation of SH that is formed during  $\text{H}^\bullet$  exposure by surface hydrogen. The 190 K desorption state is correlated with hydrogenation by desorbing subsurface hydrogen.

structure.<sup>29</sup> Therefore, this technique provides a promising new method for investigating the active sites in HDS. Initial evidence for the enhanced activity of these defect sites in the sulfided overlayer is demonstrated in Figure 7a. Examination of the  $\text{H}_2$  TPRS shows a new, low-temperature desorption state near 230 K for low sulfur defect coverages indicating hydrogen desorption is facilitated.

## Conclusions

Gas-phase hydrogen radicals remove adsorbed sulfur from the Ni(100) surface by three pathways. During hydrogen radical exposure, desulfurization occurs by an Eley–Rideal mechanism. After exposure,  $\text{H}_2\text{S}$  desorbs at 150 and 190 K in subsequent TPRS experiments. The 150 K peak  $\text{H}_2\text{S}$  is formed by hydrogen addition to an SH intermediate created during hydrogen radical exposure. Reaction of adsorbed sulfur with desorbing subsurface hydrogen leads to the 190 K TPRS peak. These three desulfurization mechanisms are illustrated in Figure 11. Because gas-phase hydrogen radicals can reproducibly create defects in a saturated sulfur monolayer, new possibilities for fundamental mechanistic studies of HDS catalysts are now available.

**Acknowledgment.** This work was supported by D.O.E. grant number DE-FG02-91ER1490, and the funding is greatly appreciated. We also thank our machinist, Albert Wilson, for his aid in the construction and modification of our UHV equipment.

## References and Notes

- (1) Hegedus, L. L.; McCabe, R. W. *Catalyst Poisoning*, Dekker: New York, 1984.
- (2) Progress in Catalyst Deactivation; Figueiredo, J. L., Eds.; Martinus Nijhoff, 1982.
- (3) (a)  $\text{H}_2\text{S}$  on Ni(111): Yang, H.; Whitten, J. L. *Surf. Sci.* **1997**, 370, 136. (b) Rh(100): Hedge, R. I.; White, J. M. *J. Phys. Chem.* **1986**, 90, 296. (c) Pt(111): Koestner, R. J.; Salmeron, M.; Kollin, E. B.; Gland, J. L. *Surf. Sci.* **1986**, 172, 668. (d) Cu(111): Campbell, C. T.; Koel, B. E. *Surf. Sci.* **1987**, 183, 100.
- (4) Koestner, R. J.; Salmeron, M.; Kollin, E. B.; Gland, J. L. *Chem. Phys. Lett.* **1986**, 125, 134.
- (5) Fisher, G. *Surf. Sci.* **1979**, 87, 215.
- (6) Gland, J. L.; Kollin, E. B.; Zaera, F. *Langmuir* **1988**, 4, 118.
- (7) Son, K. A.; Gland, J. L. *J. Am. Chem. Soc.* **1996**, 118, 10505.
- (8) Capitano, A. T.; Gland, J. L. *J. Phys. Chem.* **1998**, 102, 2563.
- (9) (a) Cyclohexene on Ni(100): Son, K. A.; Mavrikakis, M.; Gland, J. L. *J. Phys. Chem.* **1995**, 99, 6270. (b) ethylene on Ni(100): Daley, S. P.; Utz, A. L.; Trautman, T. R.; Ceyer, S. T. *J. Am. Chem. Soc.* **1994**, 116, 6001.
- (10) Takehiro, N.; Mukai, K.; Tanaka, K. *J. Chem. Phys.* **1995**, 103, 1650.
- (11) Kammler, Th.; Kuppers, J. *Chem. Phys. Lett.* **1997**, 267, 391.
- (12) Johnson, A. D.; Daley, S. P.; Utz, A. L.; Ceyer, S. T. *Science* **1992**, 257, 223.
- (13) Bischler, U.; Bertel, E. *J. Vac. Sci. Technol. A* **1993**, 11, 458.
- (14) Glines, A. M.; Anton, A. B. *Surf. Sci.* **1993**, 286, 122.
- (15) National Institute of Standards and Technology worldwide web site, <http://webbook.nist.gov/chemistry/>, and comparison to fragmentation patterns obtained in our mass spectrometer.
- (16) Zhou, Y.; White, J. M. *Surf. Sci.* **1987**, 183, 363.
- (17) Johnson, A. D.; Maynard, K. J.; Daley, S. P.; Yang, Q. Y.; Ceyer, S. T. *Phys. Rev. Lett.* **1991**, 67, 927.
- (18) Christman, K.; Schober, O.; Ertl, G.; Neumann, M. *J. Chem. Phys.* **1974**, 60, 4528.
- (19) Rieder, K. H.; Wilsch, H. *Surf. Sci.* **1983**, 131, 245.
- (20) Huntley, D. R. *Surf. Sci.* **1990**, 240, 13.
- (21) Capitano, A. T.; Gabelnick, A. M.; Gland, J. L. *Surf. Sci.* **1998**, 29, 479.
- (22) (a) Weinberg, W. H. *Acc. Chem. Res.* **1996**, 29, 479. (b) Teplyakov, A. V.; Bent, B. E. *J. Chem. Soc., Faraday Trans.* **1995**, 91, 3645.
- (23) Haug, K. L.; Burgi, T.; Trautman, T. R.; Ceyer, S. T. *J. Am. Chem. Soc.* **1998**, 120, 8885.
- (24) Alefeld, G.; Volkl, J. *Hydrogen in Metals I*, Springer-Verlag: Berlin, 1978.
- (25) (a) Chorkendorff, I.; Russell, J. N.; Yates, J. T., Jr. *Surf. Sci.* **1987**, 182, 375. (b) Comsa, G.; David, R.; Rendulic, K. D. *Phys. Rev. Lett.* **1977**, 38, 775.
- (26) Baca, A. G.; Schulz, M. A.; Shirley, D. A. *J. Chem. Phys.* **1984**, 81, 86304.
- (27) (a) Li, S. Y.; Rodriguez, J. A.; Hrbek, J.; Huang, H. H.; Xu, G. Q. *J. Vac. Sci. Technol. A* **1997**, 15, 1692. (b) Li, S. Y.; Rodriguez, J. A.; Hrbek, J.; Huang, H. H.; Xu, G. Q. *Surf. Sci.* **1996**, 366, 29.
- (28) (a) McIntyre, N. S.; Spevack, P. A.; Beamson, G.; Briggs, D. *Surf. Sci. Lett.* **1990**, 237, L390. (b) Lince, J. R.; Stewart, T. B.; Hills, M. M.; Fleischauer, P. D. *Surf. Sci.* **1989**, 210, 387. (c) Davis, S. M.; Carver, J. C. *Appl. Surf. Sci.* **1984**, 20, 193.
- (29) Kammler, Th.; Wehner, S.; Kuppers, J. *Surf. Sci.* **1995**, 125.